

DAMAGE EVOLUTION IN THE ANISOTROPIC RANGE VARIABLE MODEL OF NANOPILLAR ARRAY

Tomasz Derda

*Institute of Mathematics, Czestochowa University of Technology
Czestochowa, Poland
tomasz.derda@im.pcz.pl*

Abstract. We study mechanical-damage avalanches occurring in axially loaded nanopillars located in the nodes of the supporting square lattice. Nanopillars are treated as fibres in the framework of the stochastic Fibre Bundle Model and they are characterised by random strength thresholds. Once an element crashes, its load is transferred to the other intact elements according to a given load transfer rule. In this work we use a modified range variable model including an anisotropic-stress-transfer function. Avalanches of broken nanopillars, critical loads and clusters of damaged nanopillars are analysed by varying both the anisotropy and effective range coefficients.

Keywords: *nanopillars, fibre bundle model, damage mechanics, anisotropy*

Introduction

Fractures and damages of heterogeneous materials are common but usually undesirable phenomena. These processes attract much attention from the scientific community because of the broad area of technological applications of such materials [1-3]. It is difficult to describe fracture processes by means of statistical models because of complex relations between failures and the subsequent transfer of stresses. Nevertheless, several models have been proposed, among them the family of Fibre Bundle Models (FBM) plays a crucial role [4]. Although FBMs are simple, they capture the most important properties of material damage and breakdown.

In this work we employ the FBM approach to analyse the failure progress in arrays of nanopillars assembled perpendicularly to a flat substrate [5]. Such an arrangement is applied in the systems of micromechanical sensors.

It is worth analysing the evolution of mechanical damage of nano-sized pillars. This paper is inspired by compressive and tensile experiments performed on metallic micro- and nanopillars that confirm a significant strength increase via the size reduction of the sample [6, 7]. Thus, the arrays of free-standing nanopillars can be used as components in the fabrication of micro- and nano-electromechanical systems, micro-actuators or optoelectronic devices [6, 8].

1. Anisotropic range variable model

The system is composed of $N = L \times L$ nanopillars located in the nodes of square lattice of side length L . Each nanopillar x_i is characterised by its critical load σ_{th}^i , which is a strength threshold of the given pillar. Because of various defects during the fabrication process the pillar-strength-thresholds σ_{th}^i , $i = 1, 2, \dots, N$ are independent quenched random variables. It is assumed that the randomness of pillar-strength-thresholds σ_{th}^i , $i = 1, 2, \dots, N$ reflects the disorder of heterogeneous material. In this paper we employ uniform distribution of pillar-strength-thresholds with the probability density and distribution functions $p(\sigma_{th}) = 1$, $P(\sigma_{th}) = \sigma_{th}$. The strength-thresholds are drawn from the interval $[0, 1]$. Under the load σ_i exceeding strength-threshold σ_{th}^i the pillar is instantaneously and irreversibly damaged.

Initially all the pillars are intact, which corresponds to a zero load. Then the set of pillars is subjected to a quasi-statically increased external load F . In this approach longitudinal load F is the control parameter of the model. The increase of F is uniform for all intact pillars and it stops immediately when the weakest intact pillar crashes. After this destruction the load carried by the damaged pillar is redistributed to the other intact pillars.

In this work we employ an idea of variable range of interaction proposed by Hidalgo et al. [9]. Due to the substrate elasticity we introduce anisotropy in stress transfer, so the stress-transfer function has the following form:

$$G(r_{ij}, \gamma, \alpha) = \frac{r_{ij}^{-\gamma}(\alpha)}{\sum_{i \in I} r_{ij}^{-\gamma}(\alpha)} \quad (1)$$

Here, γ is an adjustable parameter and I denotes the set of all intact pillars. In the original work [9] r_{ij} denotes distance between the intact element i and the damaged element j . Modifying r_{ij} by an anisotropy coefficient α we obtain the formula for relative distance:

$$r_{ij}(\alpha) = \sqrt{\left(\frac{x_i - x_j}{\alpha}\right)^2 + (y_i - y_j)^2} \quad (2)$$

Coefficient α is a measure of stress transfer anisotropy, i.e. $\alpha = 1$ corresponds to the isotropic model and $\alpha > 1$ represents the stress transfer to pillars in the x -direction is α times faster than the transfer in the y -direction. It is necessary to note that this paper is in the spirit of work [10], where a somewhat different anisotropic load sharing model has been proposed in reference to a generalised discrete model.

The presented model ensures load transfer from the broken pillar to all intact pillars in the system, so the range of interaction overlays the entire system. However, the effective range of interaction depends on parameter γ . The limits $\gamma \rightarrow 0$ and $\gamma \rightarrow \infty$ correspond to two extreme rules of load sharing, namely global (GLS) and local (LLS). The GLS rule represents mean-field approach with long-range interactions between pillars. After a pillar breaks, its load is equally redistributed to all the remaining elements irrespective of their distances from the damaged element. Contrary to the GLS, in the LLS rule only short-range interactions are assumed. In this scheme the load from the broken element is transferred to neighbouring elements only, usually to the nearest ones. From the equation (1) it is seen that an increasing γ reduces the effective range of interaction. Exemplary results of the load transfer from the broken pillar to its nearest neighbours are presented in Table 1. Different values of γ and α are examined within both the GLS and LLS rules and it is assumed that only one pillar breaks, whereas other pillars stay intact.

Table 1

**The percentage of load redistributed to the nearest neighbours of the broken pillar.
Example for the system of 48×48 pillars. Coordinates of the broken pillar: (24,24)**

Load transfer scheme			Percentage of load transferred to:			
			neighbour in the x-direction	neighbour in the y-direction	four nearest neighbours	
GLS			0.043	0.043	0.174	
Range variable model with isotropic/anisotropic load transfer	$\gamma = 1$	$\alpha = 1$	0.605	0.605	2.420	
		$\alpha = 2$	0.885	0.443	2.656	
		$\alpha = 3$	1.138	0.379	3.034	
	$\gamma = 2$	$\alpha = 1$	4.302	4.302	17.209	
		$\alpha = 2$	8.379	2.095	20.947	
		$\alpha = 3$	11.884	1.320	26.410	
	$\gamma = 4$	$\alpha = 1$	16.605	16.605	66.419	
		$\alpha = 2$	37.947	2.371	80.638	
		$\alpha = 3$	43.411	0.536	87.893	
	$\gamma = 8$	$\alpha = 1$	23.357	23.357	93.427	
		$\alpha = 2$	49.416	0.193	99.218	
		$\alpha = 3$	49.775	0.008	99.564	
	$\gamma = 10$	$\alpha = 1$	24.203	24.203	96.811	
		$\alpha = 2$	49.866	0.049	99.830	
		$\alpha = 3$	49.948	0.001	99.898	
	LLS			25.000	25.000	100.000

The load transfer increases stress on the intact pillars. This increasing stress may cause other failures and then subsequent transfers followed by possible failures.

If the load transfer does not trigger further failures, a stable state is achieved. Then the external load F has to be increased with an amount as small as to provoke damage of the weakest intact pillar. It can initiate an avalanche of failures. The loading process is continued until the whole array of pillars collapses.

2. Analysis of the simulation results

Computer simulations were realised for different values of γ and α , and system sizes $N = 48 \times 48$, $N = 128 \times 128$. In order to obtain reliable statistics we have performed at least 2×10^3 simulations for the each variant of the former system size.

When the system is subjected to a quasi-statically increased external load the cascades of simultaneous pillar crashes appear. These pillar failures are similar to avalanches occurring in snow or sand movement. Due to this similarity, the number of crashed pillars under an equal external load is called an avalanche (Δ). In other words, the avalanche is the number of destroyed pillars between two consecutive external load increments.

The final stage of the damage process is the appearance of catastrophic (critical) avalanche (Δ_c) which contains all still undestroyed pillars. This complete breakdown of the system is induced by the total critical load F_c .

The first problem investigated here is the distribution of avalanche sizes. Let $D(\Delta)$ denote the number of avalanches of size Δ . Figure 1 illustrates the avalanche size distributions for $\gamma \in \{2, 4, 8\}$ and $\alpha = 2$. It turns out that for $\gamma = 2$ and $\gamma = 4$ distribution of avalanche sizes follows a power law:

$$D(\Delta) \propto \Delta^{-\tau} \quad (3)$$

with exponents $\tau \approx 2.75$ and $\tau \approx 3.4$, respectively. Value of exponent for the system with effective long range interactions ($\gamma = 2$) is close to $\tau \approx 2.5$, which is a universal mean-field exponent for the GLS rule. As it can be seen, the most abrupt way of system destruction is represented in arrays with effective short-range interactions ($\gamma = 8$). In that case departure from the power law behaviour is observed. It should be noted that critical avalanches are omitted in Figure 1.

Although during the damage process the load of individual pillars in the system is mostly unequal (with the exception of the GLS rule), it is convenient to scale the load F by the initial system size $\sigma = F/N$. Such scaled results are presented in Figure 2 which shows dependence between mean critical load $\langle \sigma_c \rangle = \langle F_c \rangle / N$ and values of anisotropy coefficient α for different γ . We have noticed that systems with effective long-range interactions ($\gamma = 1$ and $\gamma = 2$) are almost insensitive on α changes. The results obtained for $\gamma = 1$ and different α are equal to each other with an accuracy to three decimal places ($\langle \sigma_c \rangle = 0.251$). It is worth mention-

ing that for the GLS rule $\langle \sigma_c \rangle$ asymptotically tends to 0.25 which is close to the results obtained for $\gamma = 1$ and $\gamma = 2$. Influence of anisotropy is more pronounced for $\gamma = 4$: $\langle \sigma_c \rangle$ decreases nearly linear with the increase of α . When the effective short-range interactions ($\gamma = 8, 10, 12$) are considered and α grows three intervals can be distinguished in $\langle \sigma_c \rangle$ changes: decrease, small increase and again decrease. From Figure 2 it is also seen that the bigger the effective range of interactions, the stronger the system. This ordering is preserved for consecutive values of anisotropy coefficient α .

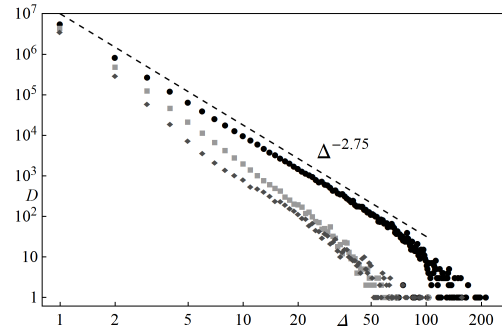


Fig. 1. The avalanche size distributions for the systems with anisotropy coefficient $\alpha = 2$ and different values of γ parameter: $\gamma = 2$ (circles), $\gamma = 4$ (squares), $\gamma = 8$ (diamonds). The results are obtained from 10 000 independent samples for each γ parameter. Size of the system $N = 48 \times 48$ pillars

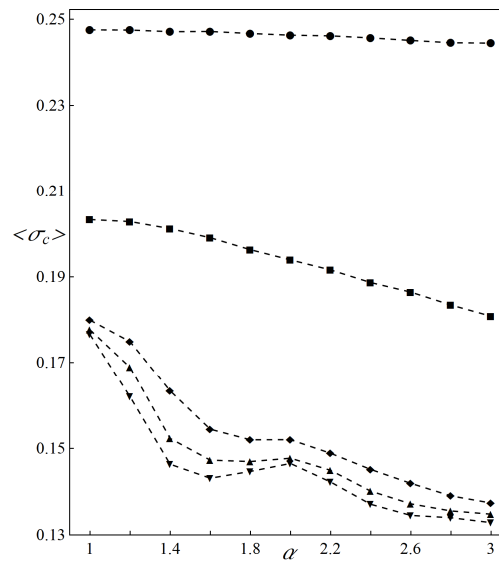


Fig. 2. The mean critical load σ_c versus the anisotropy coefficient α for different values of γ : $\gamma = 2$ (circles), $\gamma = 4$ (squares), $\gamma = 8$ (diamonds), $\gamma = 10$ (up triangles), $\gamma = 12$ (down triangles). The results are obtained from at least 2000 samples for each presented value. Size of the system $N = 48 \times 48$ pillars

Under the influence of critical load the catastrophic avalanche occurs breaking all the remaining intact pillars. Dependence between the scaled mean sizes of critical avalanches and values of anisotropy coefficient is illustrated in Figure 3. Here, compared to Figure 2, decreases/increases correspond to increases/decreases. It is important to remark, that under the GLS rule $\langle \Delta_c \rangle / N \rightarrow 0.5$.

Critical avalanche has its own self-sustained dynamics related to the stress redistribution only. During the critical avalanche a series of sub-avalanches appear. Such an avalanche, also called inclusive avalanche [11], is the number of damaged pillars per step of internal stress redistribution. Figure 4 illustrates distribution of inclusive avalanches for three different effective ranges of interactions and anisotropy coefficient $\alpha = 2$. Systems with effective long-range interactions ($\gamma = 2$) are characterised by distribution similar to that reported for the GLS rule [12]. For $\gamma = 2$ and $\gamma = 4$ distribution of medium-size sub-avalanches is close to power law. On the other hand, sub-avalanche size distribution for the systems with effective short-range interactions ($\gamma = 8$) is clearly non-trivial.

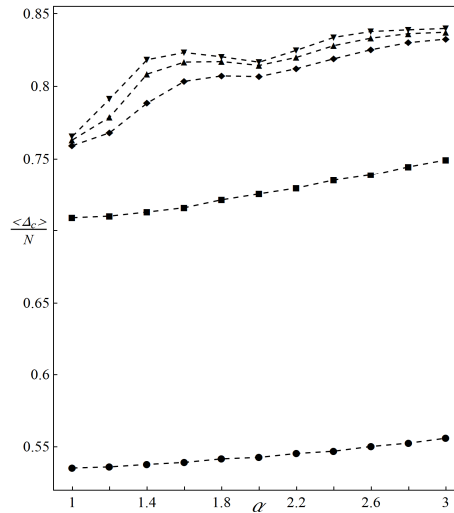


Fig. 3. The mean size $\langle \Delta_c \rangle$ of the critical avalanche scaled by the number of pillars N versus the anisotropy coefficient α for different values of γ : $\gamma = 2$ (circles), $\gamma = 4$ (squares), $\gamma = 8$ (diamonds), $\gamma = 10$ (up triangles), $\gamma = 12$ (down triangles). The results are obtained from at least 2000 samples for each presented value. Size of the system $N = 48 \times 48$ pillars

In the following we analyse empirical distributions of critical loads σ_c and critical avalanches Δ_c . The exemplary empirical probability density functions and empirical cumulative distribution functions for these two quantities have been shown in Figures 5-8. For all investigated systems, both σ_c and Δ_c are well fitted by three-parameter skew normal distribution [13-15]. When the effective range of interactions is short, the distribution of σ_c is always negative skew. In the same situation distribution of Δ_c is positive skew. Taking into account systems with effective

long-range interactions ($\gamma = 2$) it turns out that σ_c and Δ_c have an approximately Gaussian distribution (a special case of the more generic skew normal distribution).

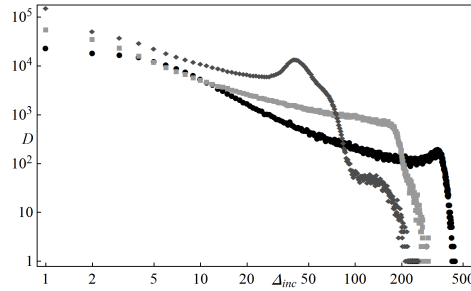


Fig. 4. The inclusive avalanche size distributions for the systems with anisotropy coefficient $\alpha = 2$ and different values of γ parameter: $\gamma = 2$ (circles), $\gamma = 4$ (squares), $\gamma = 8$ (diamonds). The results are obtained from 10 000 independent samples for each γ . Size of the system $N = 48 \times 48$ pillars

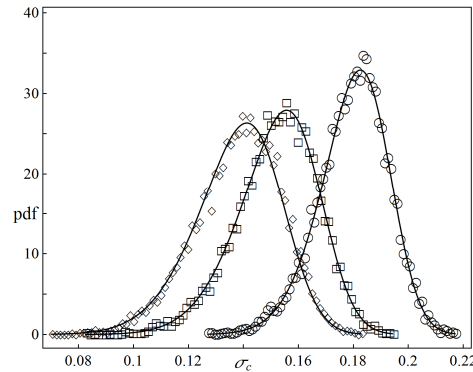


Fig. 5. The empirical probability density functions of the critical load σ_c in an array of 48×48 nanopillars and $\gamma = 8$. Three different values of α are compared: $\alpha = 1$ (circles), $\alpha = 2$ (squares) and $\alpha = 3$ (diamonds). Solid lines represent skew-normally distributed σ_c with the location, scale and shape parameters computed from the samples. Each pdf was built on 10 000 independent configurations

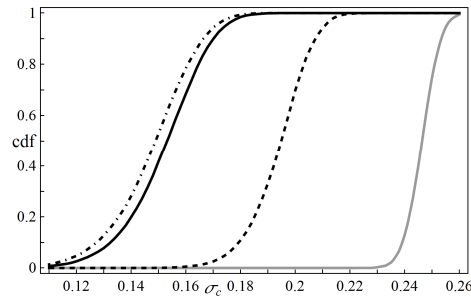


Fig. 6. The empirical cumulative distribution functions of the critical load σ_c in an array of 48×48 nanopillars and $\alpha = 2$. Four different values of γ are compared: $\gamma = 2$ (grey solid line), $\gamma = 4$ (dashed line), $\gamma = 8$ (black solid line), $\gamma = 10$ (dot-dashed line). Each cdf was built on 10 000 independent configurations

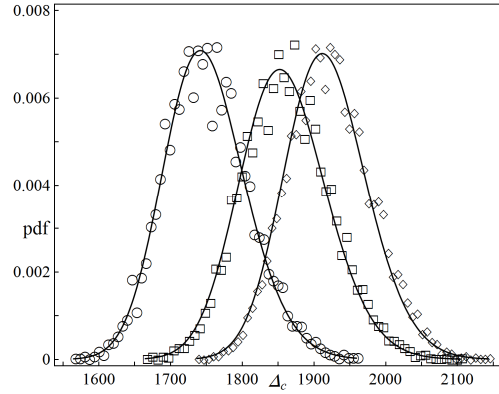


Fig. 7. The empirical probability density functions of the critical avalanche size Δ_c in an array of 48×48 nanopillars and $\gamma = 8$. Three different values of α are compared: $\alpha = 1$ (circles), $\alpha = 2$ (squares) and $\alpha = 3$ (diamonds). Solid lines represent skew-normally distributed Δ_c with the location, scale and shape parameters computed from the samples. Each pdf was built on 10 000 independent configurations

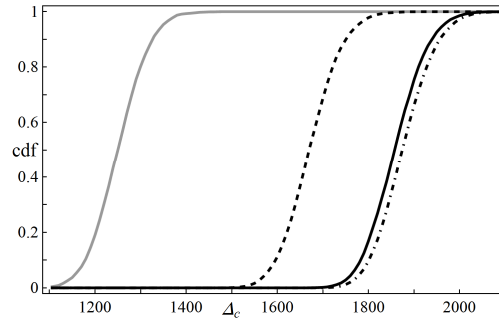


Fig. 8. The empirical cumulative distribution functions of the critical avalanche size Δ_c in an array of 48×48 nanopillars and $\alpha = 2$. Four different values of γ are compared: $\gamma = 2$ (grey solid line), $\gamma = 4$ (dashed line), $\gamma = 8$ (black solid line), $\gamma = 10$ (dot-dashed line). Each cdf was built on 10 000 independent configurations

Damage evolution can also be viewed as a nucleation process of clusters of broken pillars. Such a cluster is a group of connected damaged pillars. Two pillars are treated as connected when they are placed in the neighbouring nodes. We investigate clusters of broken pillars for systems of $N = 128 \times 128$ pillars assuming identical arrangement of identical pillars. Anisotropy of the system is characterised by $\alpha = 2$ and different γ are considered. Clusters are analysed in stable states from zero load to load just before global failure. Figure 9 presents dependence between mean cluster size and total load of the system. When $F < 2218$, so all analysed systems are still working, following ordering is noticeable: the longer the effective range of interaction, the smaller the mean cluster size. This can be explained as follows. When the effective range of interaction is long, the pillars are destroyed in a stochastic way. This is contrary to effective short-range interactions - in that case probability of damage of broken pillar neighbours increases. Figure 10 illustrates

dependence between number of clusters and total load. From this figure it is seen: the longer the effective range of interactions, the bigger the number of clusters. This is consistent with our previous explanation. In systems with the effective long range of interactions ($\gamma = 2$) the number of clusters increases, then achieves maximum and finally goes down. The behaviour in last stage results from connection of neighbouring clusters and failures of pillars adjacent to already existing clusters.

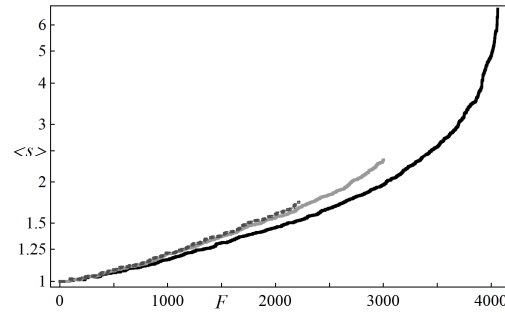


Fig. 9. The mean cluster size s versus total load F for single samples of sizes 128×128 nanopillars and $\alpha = 2$. Three different values of γ are compared: $\gamma = 2$ (black solid line), $\gamma = 4$ (light grey solid line), $\gamma = 8$ (dark grey dashed line)

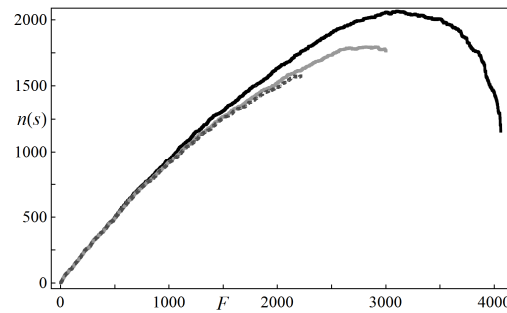


Fig. 10. The number of clusters $n(s)$ versus total load F for single samples of sizes 128×128 nanopillars and $\alpha = 2$. Three different values of γ are compared: $\gamma = 2$ (black solid line), $\gamma = 4$ (light grey solid line), $\gamma = 8$ (dark grey dashed line)

Conclusion

In summary, we have studied the failure process in longitudinally loaded arrays of nano-sized pillars with statistically distributed strength-thresholds for breakdown of an individual pillar. Load coming from destroyed pillars was transferred to other intact ones in accordance with range variable model modified by anisotropic-stress-transfer function. We have found that distribution of avalanche sizes for anisotropic systems with long and moderate effective range interactions ($\gamma = 2$ and $\gamma = 4$) is power law.

Increasing the anisotropy coefficient in the systems with effective short-range interactions three stages of changes of mean critical loads and mean catastrophic avalanches are observed. Systems with effective long-range interactions are highly resistant to changes of the anisotropy coefficient.

Based on computer simulations we have built empirical probability density and cumulative distribution functions of critical loads and critical avalanche sizes. These distributions are nicely fitted by skew normal distribution.

References

- [1] Chakrabarti B., Benguigui L.G., *Statistical Physics of Fracture and Breakdown in Disordered Systems*, Clarendon Press, Oxford 1997.
- [2] Herrmann H.J., Roux S. (eds.), *Statistical Models for the Fracture of Disordered Media*, North Holland, Amsterdam 1990 and references therein.
- [3] Alava M.J., Nukala P.K.V.V., Zapperi S., *Statistical models of fracture*, *Adv. in Physics* 2006, 55, 349-476.
- [4] Pradhan S., Hansen A., Chakrabarti B.K., *Failure processes in elastic fiber bundles*, *Rev. Mod. Phys.* 2010, 82, 499-555.
- [5] Chekurov N., Grigoras K., Peltonen A., Franssila S., Tittonen I., *The fabrication of silicon nanostructures by local gallium implantation and cryogenic deep reactive etching*, *Nanotechnology* 2009, 20, 65307. Also: <http://nanotechweb.org/cws/article/tech/37573>
- [6] Greer J.R., Jang D., Kim J.-Y., Burek M.J., *Emergence of new mechanical functionality in materials via size reduction*, *Adv. Functional Materials* 2009, 19, 2880-2886.
- [7] Huang L., Li Q.-J., Shan Z.-W., Li J., Sun J., Ma E., *A new regime for mechanical annealing and strong sample-size strengthening in body centered cubic molybdenum*, *Nature Communications* 2011, 2.
- [8] Chekurov N., *Fabrication process development for silicon micro and nanosystems*, PhD thesis, Aalto University, Helsinki, 2011. Available: <http://lib.tkk.fi/Diss/2011/isbn9789526035932/>
- [9] Hidalgo R. C., Moreno Y., Kun F., Herrmann H.J., *Fracture model with variable range of interaction*, *Phys. Rev. E* 2002, 65, 046148.
- [10] Hidalgo R.C., Zapperi S., Herrmann H.J., *Discrete fracture model with anisotropic load sharing*, *J. Stat. Mech.* 2008, P01004.
- [11] Pradhan S., Chakrabarti B.K., *Search for precursors in some model of catastrophic failures*, [in:] *Modelling Critical and Catastrophic Phenomena in Geoscience. A Statistical Approach*, P. Bhattacharyya, B.K. Chakrabarti (eds.), Springer, Heidelberg 2006, 459-477.
- [12] Domański Z., Derda T., Sczygiol N., *Statistics of critical avalanches in vertical nanopillar arrays*, *Lecture Notes in Electrical Engineering* 2014, 275, 1-11.
- [13] Azzalini A., *A class of distributions which includes the normal ones*, *Scand. J. Statist.* 1985, 12, 171-178.
- [14] Gupta A.K., Nguyen T.T., Sanqui J.A.T., *Characterization of the skew-normal distribution*, *Annals of the Institute of Statistical Mathematics* 2004, 56(2), 351-360.
- [15] Azzalini A., *The Skew-Normal and Related Families*, Cambridge University Press, 2013.